# Study of depth-dependent tetragonal distortion of quaternary AlInGaN epilayer by Rutherford backscattering/channeling*

G. Husnain†, Chen Tian-Xiang(陈田祥), Fa Tao(法 涛), and Yao Shu-De(姚淑德)‡

*State Key Laboratory of Nuclear Physics and Technology, Peking University, Beijing* 100871, *China*

(Received 7 August 2009; revised manuscript received 13 October 2009)

A 240-nm thick $Al_{0.4}In_{0.02}Ga_{0.58}N$ layer is grown by metal organic chemical vapour deposition, with an over 1-$\mu$m thick GaN layer used as a buffer layer on a substrate of sapphire (0001). Rutherford backscattering and channeling are used to characterize the microstructure of AlInGaN. The results show a good crystalline quality of AlInGaN ($\chi_{\min}$ = 1.5%) with GaN buffer layer. The channeling angular scan around an off-normal $\langle 1\bar{2}13\rangle$ axis in the $\{10\bar{1}0\}$ plane of the AlInGaN layer is used to determine tetragonal distortion $e_{\rm T}$, which is caused by the elastic strain in the AlInGaN. The resulting AlInGaN is subjected to an elastic strain at interfacial layer, and the strain decreases gradually towards the near-surface layer. It is expected that an epitaxial AlInGaN thin film with a thickness of 850 nm will be fully relaxed ($e_{\rm T} = 0$).

**Keywords:** III–V semiconductors, Rutherford backscattering and channeling, tetragonal distortion

**PACC:** 7280E, 8170C, 6855

## 1. Introduction

Group III-nitride wide band-gap semiconductors have been extensively studied due to their applications in light-emitting and electronic devices.[1,2] Compared with the ternary InGaN and AlGaN films, the quaternary AlInGaN films can offer much freedom in adjusting independently the lattice constant and band gap as discussed in other quaternary films such as InGaAsP and InGaAlP. Therefore, the quaternary AlInGaN film is a potential candidate of enhancing electrical/optical confinement and minimizing mismatch-induced strain simultaneously. Applications of AlInGaN quaternary films to light-emitting diodes (LED),[3−5] laser diodes (LD)[6,7] and filed-effect transistors[8] were demonstrated. Growth, structural and optical properties[9−12] of AlInGaN were discussed.

Rutherford backscattering and channeling (RBS/C) is a lossless quantitative technique, used to characterize composition, thickness, interface and crystalline quality of an epilayer as a function of depth.[13,14] The ion channeling proved to be a successful technique for the strain measurement of a wide variety of thin layer semiconductor systems including III-nitrides.[15] When the ion beam is directed along a high-symmetry crystal direction, a phenomenon called "channeling" occurs. The incident ion beam will undergo a series of correlated small angle scatterings, and as a result the backscattering events significantly reduce compared with the backscattering events when the ion beam is randomly directed in a direction. $\chi_{\min}$, which is the ratio of the backscattered yield when the ion beam is aligned with a crystallographic axis ($Y_{\rm A}$) to that with the random direction ($Y_{\rm R}$), is a measure of the crystalline quality of the film. RBS combined with channeling can provide useful information about, such as the crystalline quality and the defect density profile. In addition, the angular scan around an off-normal axis can determine the tetragonal distortion induced by the elastic strain in the AlInGaN. Owing to the depth sensitivity of this technique, RBS/channeling can determine the strain in the AlInGaN as a function of depth, which is impossible with conventional XRD.[16,17] The results from RBS/C are more credible than those by conventional methods such as XRD.[18,19] In the present paper, we first describe the thickness and the crystalline quality of AlInGaN with a GaN buffer layer on $Al_2O_3$ sub-

*Project supported by the National Natural Science Foundation of China (Grant No. 10875004), and the National Basic Research Program of China (Grant No. 2010CB832904).

†E-mail: husnain78@gmail.com

‡Corresponding author. E-mail: sdyao@pku.edu.cn

© 2010 Chinese Physical Society and IOP Publishing Ltd

strate, determined by the RBS/channeling technique, and then present a quantitative analysis of the strain and its depth dependence in the AlInGaN.

## 2. Experiment

Samples were grown by metal organic chemical vapour deposition (MOCVD) system. A collimated 2.0-MeV $He^+$ beam produced by 5SDH-2 Pelletron at Peking University was used for RBS/channeling measurements. The sample was mounted on a high precision (0.01°) three-axis goniometer in a vacuum chamber, so that the orientation of this sample relative to the $He^+$ beam could be precisely controlled. The backscattered particles were accepted by an Au–Si barrier detector. The detection angle was 165° and its energy resolution was about 18 keV. To study the strain related tetragonal distortion of AlInGaN, the off-normal $\langle 1\bar{2}13\rangle$ and the normal axis $\langle 0001\rangle$ are chosen to obtain 21 RBS spectra, with each corresponding to a specific tilt angle with respect to the $\langle 1\bar{2}13\rangle$ axis in the $\{10\bar{1}0\}$ plane.

## 3. Results and discussion

Random and aligned RBS spectra of the sample are shown in Fig. 1. A simulation of random spectrum performed by RUMP program[20] shows that the AlInGaN thickness is only 240 nm and GaN layer is larger than 1 $\mu$m.

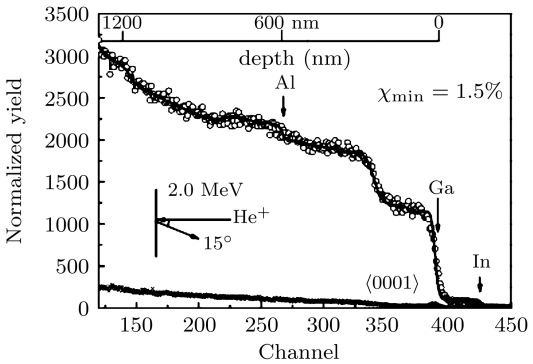



**Fig. 1.** Random (○), aligned (×) and simulated (solid line) spectra along $\langle 0001\rangle$ axis of AlInGaN/GaN/$Al_2O_3$.

The composition of epilayer is calculated to be $Al_{0.4}In_{0.02}Ga_{0.58}N$. The ratio of the backscattered yield for aligned $\langle 0001\rangle$ spectrum to that for random spectrum in the same region close to the surface called channeling, has minimum yield $\chi_{min}$ = 1.5%, which implies a low channeling rate and that $Al_{0.4}In_{0.02}Ga_{0.58}N$/GaN has a good crystalline quality (the values of $\chi_{min}$ from 1% to 2% indicate perfect crystalline quality).[21–23] Figure 1 also shows that the crystalline quality of $Al_{0.4}In_{0.02}Ga_{0.58}N$/GaN is depth-dependent. In a region close to interface (approx. 340 to 390 channels) the defect density is higher and the crystalline quality improves when approaching surface.

To analyse the strain related tetragonal distortion of the $Al_{0.4}In_{0.02}Ga_{0.58}N$, off-normal axis $\langle 1\bar{2}13\rangle$ is chosen. Figure 2 represents the aligned spectrum along the $\langle 1\bar{2}13\rangle$ axis and the random spectrum. Figure 2 has $\chi_{min}$ = 2.5% which is a little high as compared with that in Fig. 1, since the index along this axis is higher.

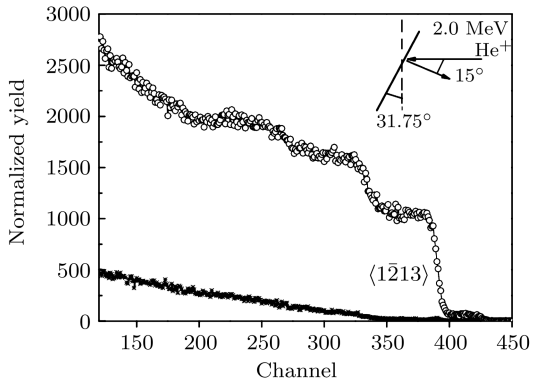



**Fig. 2.** Random (○) and aligned (×) spectra along, $\langle 1\bar{2}13\rangle$ axis of AlInGaN/GaN/$Al_2O_3$.

After the orientations of the $\{10\bar{1}0\}$ plane and the $\langle 1\bar{2}13\rangle$ axis are found, the sample is tilted step by step in the $\{10\bar{1}0\}$ plane and around the $\langle 1\bar{2}13\rangle$ axis direction from –1.8° to +2.2° with a step size of 0.2°. Thus 21 RBS spectra were obtained, with each one being subsequent to a specific tilt angle to the $\langle 1\bar{2}13\rangle$ axis in the $\{10\bar{1}0\}$ plane. Four energy windows were chosen (w1–w4) in the RBS spectra, subsequent to four regions with different depths in the $Al_{0.4}In_{0.02}Ga_{0.58}N$ as shown in Fig. 2. Using the data from the 21 RBS spectra, four angular scans around the $\langle 1\bar{2}13\rangle$ axis were obtained,[24] with each one being related to a region with specific depth determined by the energy window. For example, the angular scan subsequent to the energy window w4 is shown on the right-hand side in Fig. 3. A Gaussian function fitting is used to precisely determine the position of the dip (solid line). On the left-hand side in Fig. 3 an angular scan in the $\{10\bar{1}0\}$ plane around the $\langle 0001\rangle$ axis is shown. The centre of the $\langle 0001\rangle$ dip is not depth-dependent, because the tetragonal distortion only influences the

orientation of off-normal axes but not the ⟨0001⟩ axis. The inset in Fig. 3 schematically shows that the direction of the ⟨1$\bar{2}$13⟩ axis in the {10$\bar{1}$0} plane, which also contains ⟨0001⟩ and ⟨11$\bar{2}$0⟩ axes, is changed due to the occurrence of a tetragonal distortion. From Fig. 3, we can evaluate the angle between ⟨0001⟩ and ⟨1$\bar{2}$13⟩ axes at a depth of 229 nm (w4) of the AlInGaN.

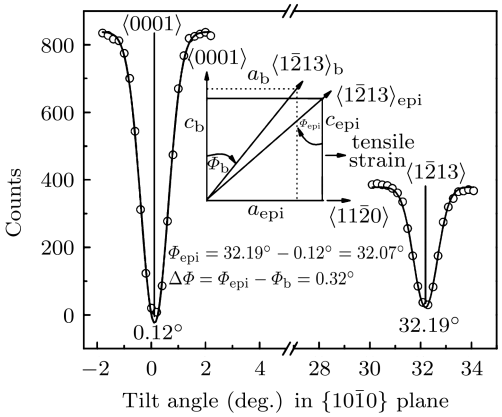



**Fig. 3.** Angular scans along the AlInGaN {10$\bar{1}$0} plane. Left: the AlInGaN ⟨0001⟩ dip and right: the AlInGaN ⟨1$\bar{2}$13⟩ dip that corresponds to the depth of 229 nm (w4). The inset shows schematically the strain related tetragonal distortion.

Since $\Phi_{epi} = \tan^{-1}(a_{epi}/c_{epi}) = 32.19° - 0.12° = 32.07°$, where $a_{epi}$ is the lattice constant of $Al_xIn_yGa_{(1-x-y)}N$. For a semiconductor alloy system, an appropriate lattice constant–composition relationship, which is often assumed to obey Vegard's law

$$a_b = a_0^{GaN}(1-x-y) + a_0^{AlN}x + a_0^{InN}y,$$

$$c_b = c_0^{GaN}(1-x-y) + c_0^{AlN}x + c_0^{InN}y,$$

where $a_0^{GaN} = 0.3189$ nm, $c_0^{GaN} = 0.5185$ nm, $a_0^{AlN} = 0.3111$ nm, $c_0^{AlN} = 0.4978$ nm, $a_0^{InN} = 0.3538$ nm, and $c_0^{InN} = 0.5706$ nm are the unstrained (relaxed) lattice constants of GaN, AlN and InN respectively. The resultant lattice constants for bulk (unstrained) $Al_{0.4}In_{0.02}Ga_{0.58}N$, $a_b = 0.3165$ nm and $c_b = 0.5115$ nm, are obtained, $\Phi_b = \tan^{-1}(a_b/c_b) = 31.75°$, as a result $\Delta\Phi = \Phi_{epi} - \Phi_b = 0.32°$, and the tetragonal distortion calculated to be $e_T = e^{\parallel} - e^{\perp} = \Delta\Phi/\sin\Phi\cos\Phi = 1.24\%$, where $e^{\parallel}$ is the parallel elastic strain. Table 1 lists the values of strain, $\Delta\Phi$ and $e_T$ at different depths, corresponding to energy windows (w1 to w4) of $Al_{0.4}In_{0.02}Ga_{0.58}N$.

**Table 1.** Strain data, $\Delta\Phi$ and $e_T$ at different depths.

| windows/nm | w1 | w2 | w3 | w4 |
|---|---|---|---|---|
| depth/nm | 29 | 96 | 163 | 229 |
| $\Delta\Phi/(°)$ | 0.25 | 0.28 | 0.305 | 0.32 |
| $e_T/\%$ | 0.98 | 1.09 | 1.18 | 1.24 |

Figure 4 shows a plot of tetragonal distortion ($e_T$) as a function of depth. The $e_T$ or ($\Delta\Phi$) values may be positive or negative, depending on whether the lattice mismatch is negative or positive, respectively.[21,25] From our results, the lattice mismatch is negative, so the $e_T$ or ($\Delta\Phi$) values are positive. It means that the AlInGaN is under tensile strain in the parallel direction ($e^{\parallel} > 0$) which results in a compressive strain in the perpendicular direction ($e^{\perp} < 0$) due to the elastic properties of the AlInGaN. The $e_T$ values are depth-dependent. The strain is higher in a region near the interface and decreases towards the surface due to the gradual reduction of the strain.

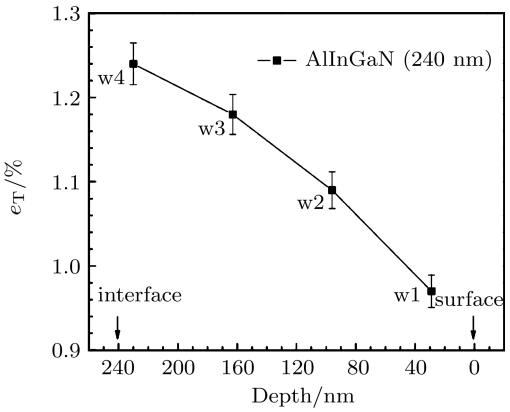



**Fig. 4.** Depth dependence of $e_T$ of the AlInGaN/GaN/$Al_2O_3$ by RBS/C.

The $e_T$ value decreases almost linearly after the thickness has exceeded 160 nm. Extrapolating this linear behaviour shows that when the AlInGaN film is 850-nm thick, then $e_T = 0$, which means that the film is fully relaxed.[26] The angular scan information obtained in the deep layer is filtered by the top layer. The real lattice strain should be larger than that measured by angular shift. In our case, such an effect may more or less lead to an lower value of $e_T$ than the real one in the deeper part of the single AlInGaN epilayer. Therefore, a fully relaxed AlInGaN layer for a thickness less than that of 850 nm is expected.

# 4. Conclusion

In this article, we presented a structural analysis of a thin film of AlInGaN/GaN on sapphire by MOCVD, prepared at Institute of Semiconductors, Chinese Academy of Sciences. We have performed experiments to find out thickness, composition, crystalline quality and depth-dependent tetragonal distortion. Results indicate that a 240-nm thick

$Al_{0.4}In_{0.02}Ga_{0.58}N$ layer has a good crystalline quality ($\chi_{min}$ = 1.5%). Hence, RBS/C again proves to be a useful technique to characterize the structure, especially since it is obligatory to study the depth dependence of the strain in $Al_{0.4}In_{0.02}Ga_{0.58}N$. The $Al_{0.4}In_{0.02}Ga_{0.58}N$ is observed to be subjected to a compressive strain at interfacial layer and the strain decreases gradually towards the near-surface layer. According to the results deduced from our measurements, it is expected that an epitaxial AlInGaN layer grown on sapphire with a thickness of 850 nm can be fully relaxed.

## Acknowledgement

We would like to express our gratitude to the Institute of Semiconductors, Chinese Academy of Sciences for providing samples.

## References

[1] Zhang J M, Zou D S, Xu C, Zhu Y X, Liang T, Da X L and Shen G D 2007 *Chin. Phys.* **16** 1135

[2] Liu N X, Wang H B, Liu J, Niu N H, Han J and Shen G D 2006 *Acta Phys. Sin.* **55** 1424 (in Chinese)

[3] Asif Khan M, Yang J W, Simin G, Gaska R, Shur M S, Zur Loye H C, Tamulaitis G and Zukauskas A 2000 *Appl. Phys. Lett.* **76** 1161

[4] Zhang J P, Yang J, Simin G, Shatalov M, Asif Khan M, Shur M S and Gaska R 2000 *Appl. Phys. Lett.* **77** 2668

[5] Chitnis A, Kumar A, Shatalov M, Adivarahan V, Lunev A, Yang J W, Simin G, Asif Khan M, Gaska R and Shur M 2000 *Appl. Phys. Lett.* **77** 3800

[6] Shatalov M, Chitnis A, Adivarahan V, Lunev A, Zhang J, Yang J W, Fareed Q, Simin G, Zakheim A, Asif Khan M, Gaska R and Shur M S 2000 *Appl. Phys. Lett.* **78** 817

[7] Hirayama H, Kinoshita A, Yamabi T, Enomoto Y, Hirata A, Araki T, Nanishi Y and Aoyagi Y 2002 *Appl. Phys. Lett.* **80** 207

[8] Chen C H, Huang L Y, Chen Y F, Jiang H X and Lin J Y 2002 *Appl. Phys. Lett.* **80** 1397

[9] Yang L, Takashi E, Hiroyasu I and Takashi J 2003 *J. Cryst. Growth* **259** 245

[10] Liu J P, Zhang B S, Wu M, Li D B, Zhang J C, Jin R Q, Zhu J J, Chen J, Wang J F, Wang Y T and Yang H 2004 *J. Cryst. Growth* **260** 388

[11] Shang J Z, Zhang B P, Wu C M, Cai L E, Zhang J Y, Yu J Z and Wang Q M 2008 *Appl. Surf. Sci.* **255** 3350

[12] Shang J Z, Zhang B P, Mao M H, Cai L E, Zhang J Y, Fang Z L, Liu B L, Yu J Z, Wang Q M, Kusakabe K and Ohkawa K 2009 *J. Cryst. Growth* **311** 474

[13] Chu W K, Mayer J W and Nicolet M A 1978 *Backscattering Spectrometry* (New York: Academic)

[14] Feng Z X, Yao S D, Hou L N and Jin R Q 2005 *Nucl. Instrum. Methods Phys. Res.* B **229** 246

[15] Alves E, Pereira S, Correia M R, Pereira E, Sequeira A D and Franco N 2002 *Nucl. Instrum. Methods Phys. Res.* B **190** 560

[16] Wu M F, Vantomme A, Hogg S M, Pattyn H, Langouche G, Stricht W V, Jacobs K and Moerman I 1999 *Appl. Phys. Lett.* **74** 365

[17] Wu M F, Yao S D, Vantomme A, Hogg S M, Langouche G, Li J and Zhang G Y 1999 *J. Vac. Sci. Technol.* B **17** 1502

[18] Lorenz K, Franco N, Alves E, Watson I M, Martin R W and O'Donnell K P 2006 *Phys. Rev. Lett.* **97** 085501

[19] Lu Y, Cong G W, Liu X L, Lu D C, Wang Z G and Wu M F 2004 *Appl. Phys. Lett.* **85** 5562

[20] Doolittle L R 1985 *Nucl. Instrum. Methods Phys. Res.* B **9** 344

[21] Wu M F, Chen C C, Zhu D Z, Zhou S Q, Vantomme A, Langouche G, Zhang B S and Yang H 2002 *Appl. Phys. Lett.* **80** 4130

[22] Ding Z B, Wang K, Zhou S Q, Chen T X and Yao S D 2007 *Chin. Phys. Lett.* **24** 831

[23] Ding Z B, Wu W, Wang K, Fa T and Yao S D 2009 *Chin. Phys. Lett.* **26** 086111

[24] Wu M F, Vantomme A, De Wachter J, Degroote S, Pattyn H, Langouche G and Bender H 1996 *J. Appl. Phys.* **79** 6920

[25] Wu M F, Yao S D, Vantomme A, Hogg S, Langouche G, Stricht W V, Jacobs K, Moerman I, Li J and Zhang G Y 2000 *Mater. Sci. Eng.* B **75** 232

[26] Pan C K, Zheng D C, Finstad T G, Chu W K, Speriosu V S, Nicolet M A and Barrett J H 1985 *Phys. Rev.* B **31** 1270